Understanding the Growth Mechanism of Titanium Disilicide Nanonets

Sa Zhou, Jin Xie, and Dunwei Wang*

Department of Chemistry, Merkert Chemistry Center, Boston College, 2609 Beacon Street, Chestnut Hill, Massachusetts 02467, United States

ABSTRACT The titanium disicilicate ($TiSi_2$) nanonet is a material with a unique two-dimensional morphology and has proven beneficial for energy conversion and storage applications. Detailed knowledge about how the nanonet grows may have important implications for understanding seedless nanostructure synthesis, in general, but is presently missing. Here, we report our recent efforts toward correcting this deficiency. We show that the $TiSi_2$ nanonet growth is sensitive to the nature of the receiving substrates. High-yield nanonets are only obtained on those exhibiting no or low reactivities with Si. This result indicates that Si-containing clusters deposited on the substrate surfaces play an important role in the nanonet synthesis, and we suggest they serve to initiate the growth. The morphological complexity of the nanonet depends on the precursor concentrations but not on the growth durations. More $TiCl_4$ results in nanonets with more complex structures. We understand that once a beam of a $TiSi_2$ nanonet is formed, its sidewalls are resistant to branch formation. Instead, the tip of a beam is where a branch forms. This process is driven by the reactions between Ti- and Si-containing species. Building on this understanding, we demonstrate the creation of second-generation nanonets.

KEYWORDS: titanium silicide · nanostructures · nanonets · chemical vapor deposition · seedless growth

When their electrodes are made of nanomaterials or materials with nanoscale features, energy conversion and storage devices, such as solar cells and rechargeable batteries, often exhibit new and improved properties.[1−6] Depending on the detailed processes involved, different devices benefit from the electrode innovations at the nanoscale differently. For instance, better light absorption or improved charge collection or both have been shown by solar cells containing nanowires;[7−10] faster charge and discharge rate or prolonged cycling lifetime or both have been reported when nanostructures are used for Li-ion batteries.[2,11−13] A key factor that enables these encouraging results is our ability to design and synthesize materials at the nanoscale. To advance research in these areas further, we need detailed understandings about how various chemical processes produce these nanostructures. Despite intense research efforts, however, this knowledge is limited.[5,6,14−18] The limitation is exemplified in the unique two-dimensional (2D) nanonet system that we recently studied.[19,20] Different from other hierarchical or branched nanowires (or nanorods), the structural complexity of the nanonet is confined within a flat sheet. We have demonstrated that this novel material is a promising platform for a number of applications, including solar water splitting[21−24] and Li-ion batteries.[12,13] Although our initial results suggest that the nanonet growth is governed by the nature of $TiSi_2$ crystal structures, and that higher Si-to-Ti ratios favor the 2D nanonet morphology,[19,20] a number of important questions remain unanswered. For instance, how do the initial nuclei form? What is the driving force for the branch formation? Can we control the degree of the complexity? These questions are of fundamental importance to the revelation of the detailed processes involved in the nanonet synthesis and will likely contribute to the understanding of nanostructure synthesis in general. Answers to these questions may eventually enable the development of chemistries that can produce nanomaterials with desired morphologies and properties—a grand challenge in materials chemistry—and therefore will have a profound impact on research in this field. Here, we report results that may help answer these questions. Our results show that the initiation of the nanonet growth is dependent on the type of substrates used and that the branch formation is driven by the reactions of the precursors at the growth tips. Using this understanding, we demonstrate that the complexity of the 2D structure can indeed be controlled and present the formation of second-generation nanonets.

RESULTS AND DISCUSSION

To elucidate how the initial nucleation process takes place, we first carried out a series of growths on different substrates, including Si, Si with thermally grown oxides, quartz, Ti foil, Ti foil with a Pt coating, Ti foil with a Si coating, Si with a Ni coating, and stainless steel foil. A clear trend was observed

* Address correspondence to dunwei.wang@bc.edu.

Received for review March 19, 2011 and accepted April 20, 2011.

Published online April 20, 2011
10.1021/nn201045g

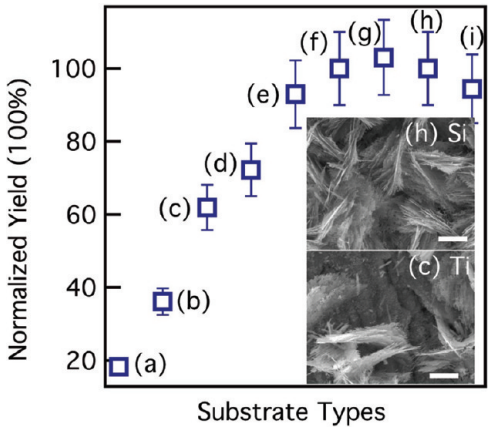

Figure 1. Comparison of $TiSi_2$ nanonet yields on different substrates. (a) Ni-coating on Si; (b) stainless steel; (c) Ti foil; (d) Ti foil with Pt coating; (e) Ti foil with Si deposition; (f) Si with thermally grown oxide; (g) quartz; (h) Si; (i) the backside of Si. The yield for each sample was normalized relative to that on the Si substrate. Two representative top-view scanning electron micrographs (SEM) of $TiSi_2$ nanonets grown on Si and Ti, respectively, are included as insets. Scale bars: 1 μm.

when the nanonet yields on these substrates were directly compared. Generally, low yields were obtained on substrates that can react with Si at elevated temperatures, as shown in Figure 1. For example, scarce $TiSi_2$ nanonets were found on Ni-coated substrates. The majority of the products were sheets that could be identified as $NiSi_x$ (see Supporting Information).[25,26] Given that the growth parameters, including the pressure (*P*), the temperature (*T*), the precursor flow rates (SiH_4 and $TiCl_4$, respectively), and the growth durations (*t*) were identical for all samples examined, we concluded that the different yields result from the differences in the nucleation processes on various substrates. We suggest that the initial nuclei leading to the production of $TiSi_2$ nanonets are made of Si, which form as a result of the SiH_4 thermal decomposition under the growth conditions. If the substrate onto which the nanonets are grown reacts with Si, the nuclei will fail to form, resulting in low or no yield of nanonets. That the yields on Si-based and Si-covered substrates (including those of amorphous and crystalline SiO_2) are comparable also supports this hypothesis because Si deposition on these surfaces is expected to be comparable. Note that the yield on Pt-coated substrates was lower than those on Si-based substrates by 30% presumably because of relatively poor adhesion of Si onto Pt surfaces.

In addition, we suggest that the growth of $TiSi_2$ nanonet is a surface process but not a gas-phase one. This means the nanostructures are not formed in the gas phase and then deposited onto the receiving substrate. Instead, they directly grow on the surface. Two pieces of evidence support this conclusion. First, no measurable differences in the yield were observed on the front side (facing up) or the back side (facing down) of a Si substrate. Second, we did not observe any

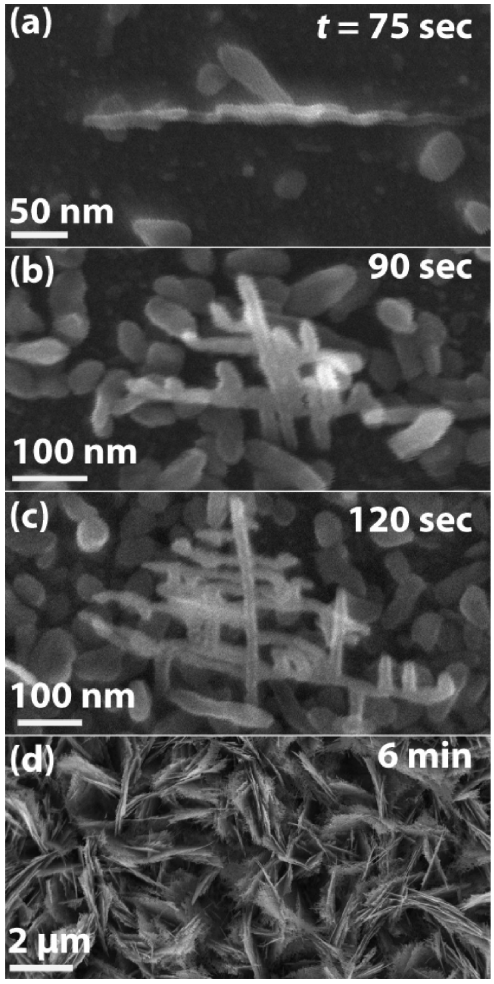

Figure 2. Evolution of $TiSi_2$ nanonets at different growth stages, varying from (a) 75 s, (b) 90 s, (c) 120 s, and (d) 6 min.

nanonets downstream away from the heated (*i.e.*, the growth) region in the growth chamber. Once produced, the nanonets were typically affixed to the substrate and could survive harsh treatments such as pressurized gas blowing or rinsing. Our previous results indicated that the nanonets form a good electrical contact to the supporting substrate with negligible resistance.[12,21,23] This means the interface between the initial growth nuclei and the substrate surface is of high quality. The property is an added benefit if the nanonets are to be used for energy-related applications, where low impedance charge transport is desired.

We next sought to examine how the nanonets form the 2D complexity by observing the different stages of a nanonet growth, at 75 s, 90 s, 120 s, and 6 min, respectively (Figure 2). According to the existing literature, at least two competing mechanisms can be used to explain the formation of a complex nanostructure. The first one involves the formation of a trunk first, from which branches grow.[16,17,27−30] Alternatively, different parts of a complex nanostructure can grow at the same time, creating the final product in a one-step reaction.[5,19,20,30,31] Our experimental observations

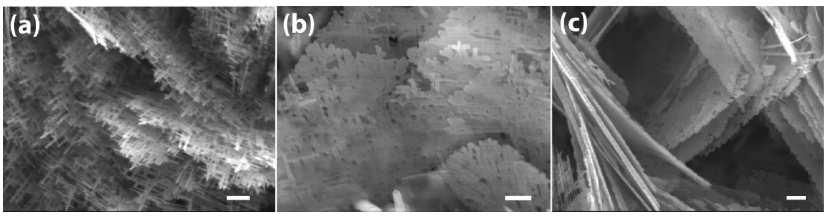

Figure 3. $TiSi_2$ nanonets of different complexities were produced under different $TiCl_4$ feeding rates: (a) 1.9 sccm, (b) 2.3 sccm, and (c) 3.0 sccm. The flow rate of SiH_4 was fixed at 50 sccm. Scale bars: 200 nm.

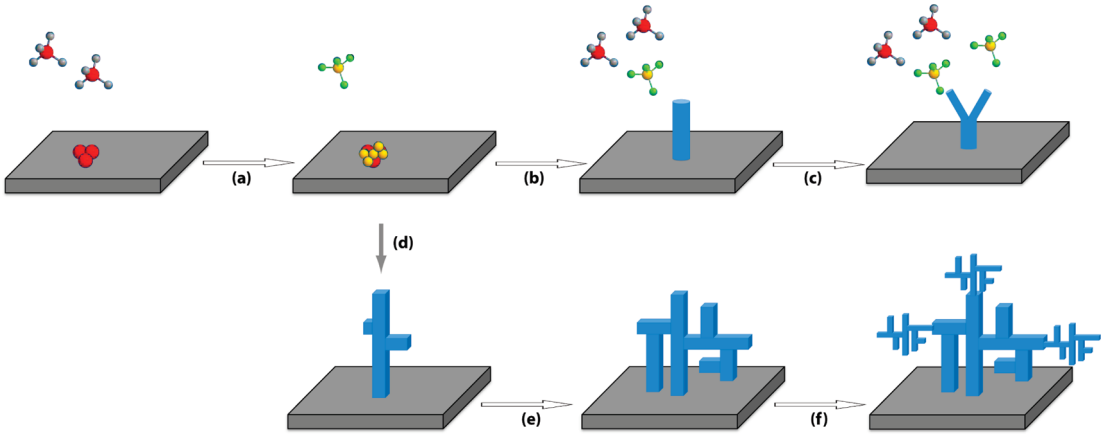

Figure 4. Schematics of the proposed mechanism governing the $TiSi_2$ nanonstructure growth. The chemistry starts with nucleus formation (a), followed by the elongation of C54 (b) and C49 (d) rods. The branching is caused by the breaking of side passivations at the growth front by Ti-containing clusters (c and e). Second-generation (2G) nanonets can be produced when the conditions change to suppress the continued growth of the original nanonets and to favor the initiation of new ones (f). Legends of color-coded balls in this schematic: red is Si; yellow is Ti; gray is H; and green is Cl.

indicated that the nanonet growth is likely governed by the second mechanism. As can be seen in Figure 2, the 2D nature of the nanonet was apparent 90 s after the growth was initiated. Throughout the growth, no branch-free trunks dominate the morphology. It suggests that all branches within a nanonet are of similar chemical reactivities. We also note the growth progresses at a relatively rapid pace. The size of a nanonet typically reaches >2 μm in 6 min. This is consistent with the report by Kim *et al.* that silicide nanowires and nanotubes grow rapidly on the surface.[32]

Another important fact was revealed by Figure 2. Although the size of a nanonet increased as the growth continued, the complexity remained unchanged. The complexity can be quasi-quantitatively defined as the ratio between the areas covered by $TiSi_2$ branches and those by the voids if a nanonet were laid flat on a surface. It was approximately 1:2 for the nanonets shown in Figure 2 and was increased to 1:1 for those shown in Figure 3a, 4:1 in Figure 3b, and higher than 9:1 in Figure 3c when different growth conditions were applied. While the SiH_4 flow rate was fixed at 50 sccm, the $TiCl_4$ flow rates varied from 1.9, 2.3, to 3.0 sccm for those in Figure 3a–c, respectively. Indeed, the nanonets shown in Figure 3c are so complex that they appear as continuous sheets, although voids as a result of the growth mechanism are still distinguishable. Significant to our discussions, the 2D nature of the highly complex nanonets remains unchanged.

We understand the result as follows. At the initial stage of the growth, nuclei mainly consisting of Si are formed. Subsequent co-deposition of Ti and Si to the nuclei leads to the formation of anisotropic $TiSi_2$ beams in a form similar to nanorods or short nanowires. Due to the passivation effect of Si on the {010} planes as a result of relatively high concentrations of SiH_4, the preferred crystal structure is C49 under the growth conditions (SiH_4 flow rate 50 sccm). As a C49 $TiSi_2$ beam continues to elongate, Ti-rich clusters occasionally break the Si passivation and lead to the formation of a branch perpendicular to the original beam. We hypothesize that the branching effect predominantly takes place at the growth front. That is, once a beam is formed, its sidewalls are passivated by Si; further deposition of Ti or Si or both onto the sidewalls is unlikely. The hypothesis is supported by the observation that the beams of a nanonet did not increase in diameters as the growth progressed. As a result of this branching mechanism, the complexity of a nanonet is determined by the growth condition (more specifically, the availability of Ti clusters). We believe Ti is the key reason for the branch formation because higher Ti concentrations produce more complex nanonets. Alternatively, one may argue that Cl in $TiCl_4$ could be

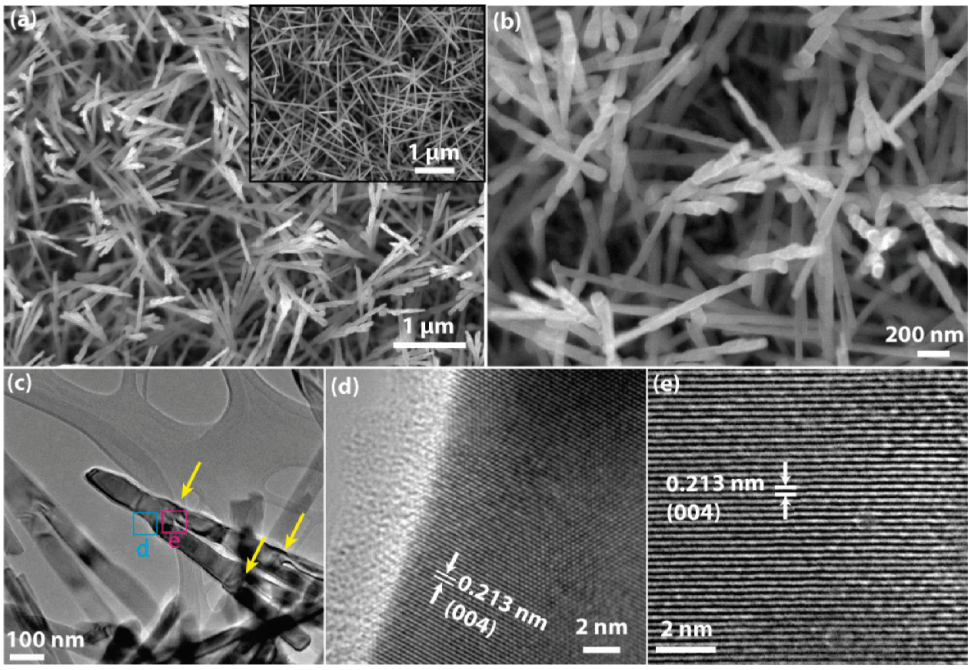

Figure 5. Splitting of $TiSi_2$ nanowires under high $TiCl_4$ flow rates. (a) Overview of nanowires with split tips by SEM. For a comparison, those without the splitting effect are shown in the inset. (b) Higher resolution SEM images reveal more details of how the nanowire tips split. (c) Further details are revealed in the TEM data. Yellow arrows point to the joints where the nanowire is split once (left arrow) and twice (right two arrows). The areas in the light blue and the purple squares are viewed under HRTEM mode, and the data are shown in (d) and (e).

the reason for the greater complexities observed when higher flow rates of $TiCl_4$ were used. This possibility was ruled out by control experiments where HCl was intentionally added, which resulted in extremely low yield of nanonets. A summary of the understanding is schematically illustrated in Figure 4.

The key new information reported here is that Ti plays an important role in producing branched nanostructures. This conclusion is further supported by the following experimental observations. As we have previously reported, the products are predominantly $TiSi_2$ nanowires (of C54 crystal structure) when SiH_4 flow rate falls below 20 sccm.[20] Under the low flow rates of SiH_4, nanowires with branches were observed when relatively high $TiCl_4$ flow rates (*e.g.*, >3.0 sccm) were used (Figure 5a−c). Several important features can be identified by examining the transmission electron microscopy (TEM) data in Figure 5c. We first direct the readers' attention to the splitting phenomenon as highlighted by the yellow arrows. That the joints appear more than once indicates the splitting is not a random process. Next we used high-resolution TEM (HRTEM) and elemental analysis (energy-dispersive spectroscopy, EDS; also see Experimental Section) to study the joint areas and measured higher Ti-to-Si ratios (0.43:1) here than other areas (0.38:1; Figure 5). Note that the ratios were lower than the stoichiometric 0.5:1 as derived from the chemical formula ($TiSi_2$) because of the surface passivation by Si. This point has been previously discussed by us.[20] Despite the differences in the Ti/Si ratios, the crystal structure of the stem and the branches was C54 without observable defects. In other words, each wire, regardless of how many times it has split, is a monolithic piece.

Presently, it is not clear why higher Ti concentration leads to the splitting of nanowires or the branching of nanonets. We hypothesize that the detailed processes may involve the breaking of Si passivation by the reaction between Ti and Si.[19,20] The intricate balance between Si depositions that are inert (on the sidewalls) and those that react with Ti (on the growth fronts) may be critical to the unique seedless growth. It is also intriguing that once the sidewalls (passivated by Si) are formed, they are resistant to further reactions, which we believe is due to the existence of Cl in the synthesis system. It is important to note that the condition windows for the various nanostructures' growths are relatively narrow, beyond which the main products are generally featureless particles made of Ti and Si.

Lastly, we show the understanding that Si-containing clusters initiate the growth and that Ti-containing ones produce complexity can help us create more complex nanostructures. After a typical nanonet growth lasting 15 min, the pressure of the reaction chamber was brought to the base level (0.5 Torr), which caused the nanonets to stop growing. Shortly afterward (15 s), the precursors (SiH_4 and $TiCl_4$) were introduced to raise the pressure to 5 Torr again. Instead of observing the previously produced nanonet continue to grow, we found new nanonets formed from the

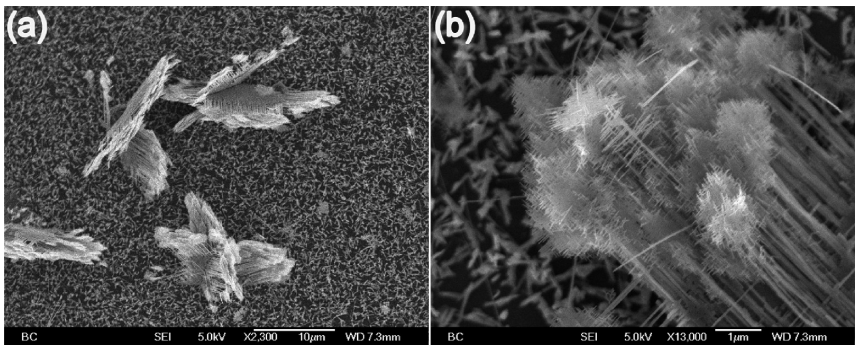

Figure 6. Creation of more complex nanonets. When the growth of nanonets was perturbed and then resumed, 2G nanonets were produced at the tips of the previously grown ones. The structures are shown under different magnifications in (a) and (b) by SEM.

beam tips (and from the tips only), creating second-generation (2G) nanonets (Figure 6). This phenomenon may be explained as follows. After the growth was stopped, the growth tips remained active. However, when the reactants were reintroduced, the previous balance between the tip growth and the side passivation no longer existed. Instead, a new balance was established, leading to the production of new nanonets. Because the tips of the previously grown nanonets were the most active, new nanonets tended to grow from there. We later discovered that the production of 2G nanonets was highly reproducible and that relatively mild changes of pressures (*e.g.*, from 5 to 4 Torr during the growth) accompanied by disruptions of the continuous feeding of the precursors could yield similar results, although the effect was less pronounced. These highly complex nanostructures are of higher surface areas than simple nanonets or nanowires and therefore may be of interest for energy-related applications.

CONCLUSIONS

Many studies on nanostructure synthesis are driven by how the resulting materials may be used for various applications. A critical challenge in this area is to produce materials with controlled compositions, crystal structures, morphologies, and properties. Seemingly elusive, this goal might be eventually achieved if we gain enough understanding on the chemistries that produce various nanostructures. Reported here were our efforts toward this goal. In line with other literature reports, we discovered that the yield of $TiSi_2$ nanonets depended on the type of substrates they were grown on, from which we concluded the growth was initiated by the formation of Si-containing clusters. We found the complexity of $TiSi_2$ nanonets did not change as a function of growth time but was only sensitive to the precursor concentrations. This observation led us to uncover the role played by Ti-containing clusters, which was to split the growth fronts. We demonstrated that this understanding could be used to produce second-generation nanonets on the tips of existing ones. The resulting materials may be useful for energy-related research owing to their unique morphological complexities and their physical and chemical properties.

EXPERIMENTAL SECTION

Material Preparation. Following the procedures reported before,[19,20] we grew $TiSi_2$ nanostructures in a home-built chemical vapor deposition (CVD) system. Note: the system is configured such that the time required for a pressure change from the base level (0.5 Torr) to 5 Torr is generally less than 15 s. For a typical growth, the reaction chamber was heated to 675 °C, and 50 sccm SiH_4 (10% in He, Voltaix) and 2 sccm $TiCl_4$ (carried by 100 sccm H_2) were delivered into the chamber. The pressure was maintained constant at 5 Torr during the growth. The duration of a typical growth was 6 min.

For the production of more complex nanonets, the reaction chamber was evacuated to the base pressure (0.5 Torr) after a growth of $TiSi_2$ nanonets. During the process, all precursor and carrier gases were kept flowing at constant rates. Shortly after the pressure reached the base level (*e.g.*, 15 s), the pressure was allowed to increase to 5 Torr again. The growth was maintained for 4 min before the system was evacuated again without precursor gases flowing. Afterward, the system was brought to room temperature for sample extractions.

The nanonet growth was also carried out on various substrates. They included Si (Wafernet, San Jose, CA), Si with thermally grown oxides (100 nm SiO_2; Wafernet), Si with Ni coating (100 nm, prepared in a sputtering system; AJA international Orion-8), stainless steel (McMaster-Carr, 0.05 mm), Ti foil (Sigma, 0.127 mm), Ti foil with Pt coating (100 nm, prepared in an e-beam evaporation system; Lesker PVD 75), quartz (Chemglass, New Jersey). The Si coating on Ti foil was achieved by exposing a Ti foil in the same CVD system used for the nanonet growth. The deposition was carried out at 675 °C for 5 min with 50 sccm SiH_4 (10% in He) and 100 sccm H_2 flowing (P_{total} = 5 Torr). The resulting Si coating was estimated to be approximately 20 nm by SEM (JEOL, JSM6340F).

Nanonet Yield Quantification. Once synthesized, the nanonets on a given supporting substrate were surveyed by the SEM. The yield was quantified by counting how many nanonets were observed in a 24 × 18 μm^2 area. For a typical experiment, more than 15 frames of SEM pictures were examined to obtain an accurate measure of the average yield. The density of nanonets on Si substrates was set as 100% for the normalized yield.

Structural Characterizations. A scanning electron microscope (JEOL, JSM6340F) and a transmission electron microscope (JEOL, JEM2010F), operating at 5 and 200 kV, respectively, were used for structural characterizations. An energy-dispersive X-ray

spectroscopy (EDS) attachment to the TEM was used to measure the chemical compositions.

Acknowledgment. This work was supported by Boston College, NSF (DMR 1055762), and Massachusetts Clean Energy Center (MassCEC). We thank Stephen Shepard at the Boston College Nanofabrication Facilities for his assistance of the metal depositions. We also thank the reviewers for their constructive comments during the review process of this manuscript.

Supporting Information Available: SEM image and XRD patterns of $NiSi_x$ nanostructures grown by reacting SiH_4 with Ni coatings on Si. This material is available free of charge *via* the Internet at http://pubs.acs.org.

REFERENCES AND NOTES

1. Hochbaum, A. I.; Yang, P. Semiconductor Nanowires for Energy Conversion. *Chem. Rev.* **2009**, *110*, 527–546.
2. Chan, C. K.; Peng, H.; Liu, G.; McIlwrath, K.; Zhang, X. F.; Huggins, R. A.; Cui, Y. High-Performance Lithium Battery Anodes Using Silicon Nanowires. *Nat. Nanotechnol.* **2008**, *3*, 31–35.
3. Huynh, W. U.; Dittmer, J. J.; Alivisatos, A. P. Hybrid Nanorod–Polymer Solar Cells. *Science* **2002**, *295*, 2425–2427.
4. Tian, B.; Zheng, X.; Kempa, T. J.; Fang, Y.; Yu, N.; Yu, G.; Huang, J.; Lieber, C. M. Coaxial Silicon Nanowires as Solar Cells and Nanoelectronic Power Sources. *Nature* **2007**, *449*, 885–889.
5. Liu, X. H.; Lin, Y. J.; Zhou, S.; Sheehan, S.; Wang, D. W. Complex Nanostructures: Synthesis and Energetic Applications. *Energies* **2010**, *3*, 285–300.
6. Bierman, M. J.; Jin, S. Potential Applications of Hierarchical Branching Nanowires in Solar Energy Conversion. *Energy Environ. Sci.* **2009**, *2*, 1050–1059.
7. Kayes, B. M.; Atwater, H. A.; Lewis, N. S. Comparison of the Device Physics Principles of Planar and Radial P–N Junction Nanorod Solar Cells. *J. Appl. Phys.* **2005**, *97*, 114302.
8. Kelzenberg, M. D.; Boettcher, S. W.; Petykiewicz, J. A.; Turner-Evans, D. B.; Putnam, M. C.; Warren, E. L.; Spurgeon, J. M.; Briggs, R. M.; Lewis, N. S.; Atwater, H. A. Enhanced Absorption and Carrier Collection in Si Wire Arrays for Photovoltaic Applications. *Nat. Mater.* **2010**, *9*, 239–244.
9. Yuan, G.; Zhao, H. Z.; Liu, X. H.; Hasanali, Z.; Zou, Y.; Levine, A.; Wang, D. Synthesis and Photoelectrochemical Study of Vertically Aligned Si Nanowire Arrays. *Angew. Chem., Int. Ed.* **2009**, *48*, 9680–9684.
10. Yuan, G.; Aruda, K.; Zhou, S.; Levine, A.; Xie, J.; Wang, D. Understanding Origin of Low Performance of Chemically Synthesized Si Nanowires for Energy Conversion. *Angew. Chem., Int. Ed.* **2011**, *50*, 2334–2338.
11. Bruce, P.; Scrosati, B.; Tarascon, J. M. Nanomaterials for Rechargeable Lithium Batteries. *Angew. Chem., Int. Ed.* **2008**, *47*, 2930–2946.
12. Zhou, S.; Liu, X. H.; Wang, D. W. Si/$TiSi_2$ Hetero-nanostructures as High Capacity Anode Material for Li Ion Batteries. *Nano Lett.* **2010**, *10*, 860–863.
13. Zhou, S.; Wang, D. W. Unique Lithiation and Delithiation Processes of Nanostructured Metal Silicides. *ACS Nano* **2010**, *4*, 7014–7020.
14. Lieber, C. M. Nanoscale Science and Technology: Building a Big Future from Small Things. *Mater. Res. Bull.* **2003**, *28*, 486–491.
15. Xia, Y. N.; Yang, P. D.; Sun, Y. G.; Wu, Y. Y.; Mayers, B.; Gates, B.; Yin, Y. D.; Kim, F.; Yan, Y. Q. One-Dimensional Nanostructures: Synthesis, Characterization, and Applications. *Adv. Mater.* **2003**, *15*, 353–389.
16. Manna, L.; Milliron, D. J.; Meisel, A.; Scher, E. C.; Alivisatos, A. P. Controlled Growth of Tetrapod-Branched Inorganic Nanocrystals. *Nat. Mater.* **2003**, *2*, 382–385.
17. Wang, D.; Qian, F.; Yang, C.; Zhong, Z. H.; Lieber, C. M. Rational Growth of Branched and Hyperbranched Nanowire Structures. *Nano Lett.* **2004**, *4*, 871–874.
18. Kanaras, A. G.; Sonnichsen, C.; Liu, H. T.; Alivisatos, A. P. Controlled Synthesis of Hyperbranched Inorganic Nanocrystals with Rich Three-Dimensional Structures. *Nano Lett.* **2005**, *5*, 2164–2167.
19. Zhou, S.; Liu, X. H.; Lin, Y. J.; Wang, D. W. Spontaneous Growth of Highly Conductive Two-Dimensional $TiSi_2$ Nanonets. *Angew. Chem., Int. Ed.* **2008**, *47*, 7681–7684.
20. Zhou, S.; Liu, X.; Lin, Y.; Wang, D. Rational Synthesis and Structural Characterizations of Complex $TiSi_2$ Nanostructures. *Chem. Mater.* **2009**, *21*, 1023–1027.
21. Lin, Y.; Zhou, S.; Liu, X.; Sheehan, S.; Wang, D. TiO_2/$TiSi_2$ Heterostructures for High-Efficiency Photoelectrochemical H_2O Splitting. *J. Am. Chem. Soc.* **2009**, *131*, 2772–2773.
22. Liu, R.; Lin, Y. J.; Chou, L.-Y.; Sheehan, S. W.; He, W.; Zhang, F.; Hou, H. J. M.; Wang, D. W. Water Splitting Using Tungsten Oxide Prepared by Atomic Layer Deposition and Stabilized by Oxygen-Evolving Catalyst. *Angew. Chem., Int. Ed.* **2011**, *50*, 499.
23. Lin, Y. J.; Zhou, S.; Sheehan, S. W.; Wang, D. Nanonet-Based Hematite Heteronanostructures for Efficient Solar Water Splitting. *J. Am. Chem. Soc.* **2011**, *133*, 2398–2401.
24. Lin, Y.; Yuan, G.; Liu, R.; Zhou, S.; Sheehan, S. W.; Wang, D. Semiconductor Nanostructure-Based Photoelectrochemical Water Splitting: A Brief Review. *Chem. Phys. Lett.* 2011, DOI: 10.1016/j.cplett.2011.03.074.
25. Decker, C. A.; Solanki, R.; Freeouf, J. L.; Carruthers, J. R.; Evans, D. R. Directed Growth of Nickel Silicide Nanowires. *Appl. Phys. Lett.* **2004**, *84*, 1389–1391.
26. Kim, C. J.; Kang, K.; Woo, Y. S.; Ryu, K. G.; Moon, H.; Kim, J. M.; Zan, D. S.; Jo, M. H. Spontaneous Chemical Vapor Growth of NiSi Nanowires and Their Metallic Properties. *Adv. Mater.* **2007**, *19*, 3637–3642.
27. Lao, J. Y.; Wen, J. G.; Ren, Z. F. Hierarchical ZnO Nanostructures. *Nano Lett.* **2002**, *2*, 1287–1291.
28. Bierman, M. J.; Lau, Y. K. A.; Jin, S. Hyperbranched PbS and PbSe Nanowires and the Effect of Hydrogen Gas on Their Synthesis. *Nano Lett.* **2007**, *7*, 2907–2912.
29. Bierman, M. J.; Lau, Y. K. A.; Kvit, A. V.; Schmitt, A. L.; Jin, S. Dislocation-Driven Nanowire Growth and Eshelby Twist. *Science* **2008**, *320*, 1060–1063.
30. Schmitt, A. L.; Higgins, J. M.; Szczech, J. R.; Jin, S. Synthesis and Applications of Metal Silicide Nanowires. *J. Mater. Chem.* **2010**, *20*, 223–235.
31. Szczech, J. R.; Jin, S. Epitaxially-Hyperbranched FeSi Nanowires Exhibiting Merohedral Twinning. *J. Mater. Chem.* **2010**, *20*, 1375–1382.
32. In, J.; Seo, K.; Lee, S.; Yoon, H.; Park, J.; Lee, G.; Kim, B. Morphology-Tuned Synthesis of Single-Crystalline V_5Si_3 Nanotubes and Nanowires. *J. Phys. Chem. C* **2009**, *113*, 12996–13001.